Available online at www.sciencedirect.com

ScienceDirect

Procedia Engineering 127 (2015) 869 – 876

Procedia Engineering

www.elsevier.com/locate/procedia

International Conference on Computational Heat and Mass Transfer-2015

Peristaltic Transport of Jeffrey NanoFluid in Curved Channels

V. K. Narla[a]*, K. M. Prasad[a], J. V. Ramanamurthy[b]

GITAM University, Department of Mathematics, Hyderabad, India
National Institute of Technology, Department of Mathematics, Warangal – 506 004, India

Abstract

The paper deals with a theoretical investigation of the transport of a Jeffrey nanofluid through two-dimensional curved channel undergoing peristalsis. The flow is investigated under the assumption of long wavelength and low Reynolds number approximations. The distribution of velocity, temperature and nanoparticles concentration are discussed for various parameters governing the flow with the simultaneous effects of Brownian motion and thermophoretic diffusion of nanoparticles.

Peer-review under responsibility of the organizing committee of ICCHMT – 2015

Keywords: nanofluid; peristalsis; curved channel

1. Introduction

Peristaltic transport has been studied with great interest by many researchers for Newtonian and non-Newtonian fluids because of its application in biology and Modern technology. The research into the fluid transport in curved geometries undergoing peristalsis is very limited. (see for example the literature [15, 6, 7, 9, 8, 11, 14, 10] and several references therein). Peristaltic transport of a nanofluid is significant method of transport in cancer treatment and applications in drug delivery. Available publications and reviews indicate that literature focusing the peristaltic transport of nanofluids are very limited (e.g., [3, 1, 2, 4, 5, 16, 12, 13]). Non-Newtonian fluids have wonderful applications in industrial and biological processes. Moreover, the importance of thermal effects of blood in the processes like oxygenation and hemodialysis makes the study about the performance of heat transfer in peristalsis very important. Considerable interest has focused on non-Newtonian fluid models as a

* Corresponding author.
E-mail address: vknarla@gmail.com

Peer-review under responsibility of the organizing committee of ICCHMT – 2015
doi:10.1016/j.proeng.2015.11.424

base fluid of nanofluids. The present work therefore analyzes the mixed convective peristaltic flow of Jeffrey nanofluid in a curved vertical channel. The governing equations contain the simultaneous effects of Brownian motion and thermophoretic diffusion of nanoparticles. The flow patterns are studied under the assumption of long wave length and the negligible flow Reynolds number approximation. Theoretical results are presented for the distribution of velocity, temperature and nanoparticles concentration.

2 Governing equations

Consider a two-dimensional motion of an incompressible viscous fluid in a curved channel of width $2a$, center O and radius R as shown in Figure 1. The flow is generated due to the transverse deflections of sinusoidal waves of small amplitude b that are imposed on the flexible walls of the channel. The inertial effects are assumed to be small. The lower and upper walls of the channels are maintained at the same temperature T_0 and concentration C_0. The equations of the channel walls are described as:

$$r = \pm h(x,t) = \pm a \pm b\, cos[2\pi(\frac{x}{\lambda} - \frac{t}{T})], \tag{1}$$

Here, x is the axial distance, a the radius of the stationary curved channel, b is the wave amplitude, λ the wave length, t the time, T the wave period, and h the radial displacement of the wave from the central line. The wavelength is large compared with the channel's width $(\frac{a}{\lambda} << 1)$.

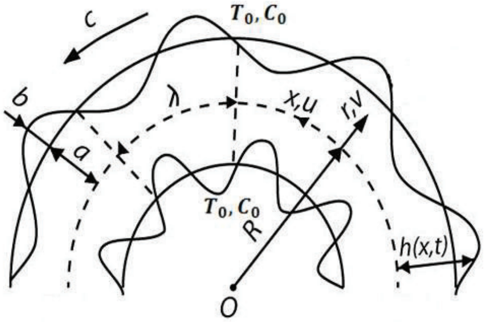

Figure 1: Peristaltic wave in curved channel.

The governing equations for the conservation of mass, momentum, energy and nanoparticles concentration for Jeffrey fluid in a curved channel can be written as:

Equation of mass conservation

$$\frac{R}{r+R}\frac{\partial u}{\partial x} + \frac{\partial v}{\partial r} + \frac{v}{r+R} = 0, \tag{2}$$

Equation of momentum conservation

$$\begin{aligned}\rho_f[\frac{\partial u}{\partial t} + (\bar{V}\cdot\nabla)u + \frac{uv}{r+R}] &= -\frac{R}{r+R}\frac{\partial p}{\partial x} + \frac{R}{r+R}\frac{\partial \tau_{xx}}{\partial x} \\ &+ \frac{1}{(r+R)^2}\frac{\partial}{\partial r}\{(r+R)^2\tau_{rx}\} + (1-C_0)\rho_f g\alpha(T-T_0) + (\rho_p - \rho_f)g\beta(C-C_0),\end{aligned} \tag{3}$$

$$\rho_f[\frac{\partial v}{\partial t} + (\bar{V}\cdot\nabla)v - \frac{u^2}{r+R}] = -\frac{\partial p}{\partial r} - \frac{\tau_{xx}}{r+R} + \frac{R}{r+R}\frac{\partial \tau_{xr}}{\partial r} + \frac{1}{r+R}\frac{\partial}{\partial r}\{(r+R)\tau_{rr}\}, \tag{4}$$

Equation of energy conservation

$$[\frac{\partial T}{\partial t}+(\overline{V}\cdot\nabla)T]=\frac{K}{(\rho c)_p}\nabla^2 T+\tau[D_B(\nabla C\cdot\nabla T)+\frac{D_T}{T_m}(\nabla T\cdot\nabla T)] +\frac{\mu}{(\rho c)_p}[4(\frac{\partial v}{\partial r})^2+(\frac{\partial u}{\partial r}+\frac{u}{r+R}+\frac{\partial v}{\partial x})^2], \tag{5}$$

Equation of nanoparticles concentration

$$[\frac{\partial C}{\partial t}+(\overline{V}\cdot\nabla)C]=D_B\nabla^2 C+\frac{D_T}{T_m}\nabla^2 T, \tag{6}$$

where

$$\overline{V}\cdot\nabla=\frac{Ru}{(r+R)}\frac{\partial}{\partial x}+v\frac{\partial}{\partial r},$$

$$\nabla^2=(\frac{R}{r+R})^2\frac{\partial^2}{\partial x^2}+\frac{1}{r+R}\frac{\partial}{\partial r}\{(r+R)\frac{\partial}{\partial r}\},$$

$$\tau_{xx}=\frac{2\mu}{1+\lambda_1}[1+\lambda_2\{\frac{\partial}{\partial t}+\frac{Ru}{r+R}\frac{\partial}{\partial x}+v\frac{\partial}{\partial r}\}](\frac{R}{r+R}\frac{\partial u}{\partial x}+\frac{v}{r+R}),$$

$$\tau_{xr}=\frac{\mu}{1+\lambda_1}[1+\lambda_2\{\frac{\partial}{\partial t}+\frac{Ru}{r+R}\frac{\partial}{\partial x}+v\frac{\partial}{\partial r}\}](\frac{\partial u}{\partial r}+\frac{R}{r+R}\frac{\partial v}{\partial x}-\frac{u}{r+R}),$$

$$\tau_{rr}=\frac{2\mu}{1+\lambda_1}[1+\lambda_2\{\frac{\partial}{\partial t}+\frac{Ru}{r+R}\frac{\partial}{\partial x}+v\frac{\partial}{\partial r}\}]\frac{\partial v}{\partial x},$$

where p, ρ_f, μ, ν, K, c_p, T, C, D_B, D_T, $\tau=\frac{(\rho c)_p}{(\rho c)_f}$, α, β, and g are the pressure, density of the fluid, dynamic viscosity, kinematic viscosity, thermal conductivity, specific heat at constant pressure, temperature, concentration, Brownian diffusion coefficient, thermophoretic diffusion coefficient, ratio of the effective heat capacity of the nanoparticle material and heat capacity of the fluid, coefficient of linear thermal expansion of the fluid, coefficient of expansion with concentration, and acceleration due to gravity. The following dimensionless variables and velocity stream function relationship are introduced:

$$x'=\frac{x}{\lambda},r'=\frac{r}{a},u'=\frac{u}{c},v'=\frac{v}{\delta c},\delta=\frac{a}{\lambda},t'=\frac{ct}{\lambda}\,h'=\frac{h}{a},\phi=\frac{b}{a},\kappa=\frac{R}{a},$$

$$L'=\frac{L}{\lambda},p'=\frac{a^2 p}{\mu c\lambda},Re=\frac{\rho_f ca}{\mu},\psi'=\frac{\psi}{ac},F=\frac{Q}{ac},\tau'_{ij}=\frac{a\tau_{ij}}{\mu c},\sigma=\frac{C-C_0}{C_0},$$

$$\theta=\frac{T-T_0}{T_0},Pr=\frac{\mu c_p}{K},Ec=\frac{c^2}{c_p T_0},Nb=\frac{\tau D_B C_0}{\nu},Nt=\frac{\tau D_T T_0}{T_m\nu},$$

$$Gr=\frac{\alpha g T_0 a^2(1-C_0)}{c\nu},Gc=\frac{(\rho_p-\rho_f)\beta g C_0 a^2}{c\mu},u=\frac{\partial\psi}{\partial r},v=-\frac{\kappa}{r+\kappa}\frac{\partial\psi}{\partial x}.$$

In which Re is the Reynolds number, F is the volume flow rate, δ is the wave number, ϕ is the amplitude ratio or the occlusion parameter, κ is the curvature parameter, P_r is the Prandtl number, E is the Eckert number, Nb is the Brownian motion parameter, Nt is the thermophoresis parameter, Gr is the thermal buoyancy parameter or local temperature Grashof number, Gc is the concentration buoyancy parameter or local nanoparticle Grashof number. The equations 2 to 6 under the assumption of long wave length and low Reynolds number are expressed in the following dimensionless form (after dropping the primes):

$$\frac{\partial}{\partial r}[\frac{1}{r+\kappa}\frac{\partial}{\partial r}\{\frac{(r+\kappa)^2}{1+\lambda_1}(\frac{\partial^2\psi}{\partial r^2}-\frac{1}{r+\kappa}\frac{\partial\psi}{\partial r})\}+(r+\kappa)(Gr\,\theta+Gc\,\sigma)]=0, \quad (7)$$

$$\frac{1}{Pr}(\frac{\partial^2\theta}{\partial r^2}+\frac{1}{r+\kappa}\frac{\partial\theta}{\partial r})+Ec(\frac{\partial^2\psi}{\partial r^2}-\frac{1}{r+\kappa}\frac{\partial\psi}{\partial r})^2+Nb(\frac{\partial\theta}{\partial r}\frac{\partial\sigma}{\partial r})+Nt(\frac{\partial\theta}{\partial r})^2=0, \quad (8)$$

$$\frac{\partial^2\sigma}{\partial r^2}+\frac{1}{r+\kappa}\frac{\partial\sigma}{\partial r}+\frac{Nt}{Nb}(\frac{\partial^2\theta}{\partial r^2}+\frac{1}{r+\kappa}\frac{\partial\theta}{\partial r})=0, \quad (9)$$

the corresponding dimensionless boundary conditions are given by

$$\psi=\pm\frac{F}{2},\ \frac{\partial\psi}{\partial r}=0,\ \theta=0,\ \sigma=0,\ \text{at}\ r=\pm h=\pm(1+\phi\,cos2\pi(x-t)) \quad (10)$$

The boundary conditions at the walls are flow boundary condition and no-slip boundary condition. The temperature and nanoparticles concentration values at both the channel walls are assumed to be zero. The flow condition or flux condition states that the flow rate flow rate is equivalent to normal velocity of the fluid at the wall. The other condition states that the tangential fluid velocity is zero at the channel walls.

The relation between volume flow rate and time averaged flow rate is ([14])

$$F(x,t)=Q_T+2(h(x,t)-1). \quad (11)$$

3. Numerical results and discussion

The coupled nonlinear differential equations (7) - (9) subject to boundary conditions (10) are solved for stream function ψ, temperature distribution function θ, and nanoparticles concentration distribution function σ by employing the built in routine for solving nonlinear boundary value problems via shooting method using the computational software Mathematica.

The coupled nonlinear differential equations (7) - (9) subject to boundary conditions (10) are solved for stream function ψ, temperature distribution function θ, and nanoparticles concentration distribution function σ by employing the built in routine for solving nonlinear boundary value problems via shooting method using the computational software Mathematica.

3.1 Axial velocity

Figure 3 shows the behavior of velocity profile under the variation of curvature parameter κ, Jeffrey fluid parameter λ_1, local temperature Grashof number Gr, local nanoparticle Grashof number Gc, Brownian motion parameter Nb, and thermophoresis parameter Nt. It is noticed from figure 3 that for small values of κ (curved channel) the velocity profiles are not symmetric about central line of the channel $r = 0$ and maximum velocity occurs in the region close to lower wall. However, for large values of κ (straight channel) the velocity profiles are symmetric about $r = 0$ and maximum velocity attains at the central line of the channel. The effect of material parameter λ_1 in a curved channel is depicted in figure 3, viscoelastic fluids are characterized by the fluid with large relaxation time. The parameter λ_1 is the ratio of relaxation to retardation time for a Jeffrey fluid. It is found that the velocity increases with the increase in λ_1 in the region close to the lower wall [−1.5,−0.5] and decreases in the region close to the upper wall. In other wards, the increase in λ_1 increases flow resistance due to small relaxation time in the upper part of the channel and decreases flow resistance due to large relaxation time in the lower part of the curved channel. In figure 3, the effect of Gr is discussed. It is observed that an increase in Gr increases velocity in the upper side of the curved channel where buoyancy force due to temperature gradient dominates the viscous force while it contributes in decreasing velocity as viscous forces are dominated in the lower side of the curved channel. Figure 3 depicts that the velocity decreases with an increase in Gc at the upper wall side and the velocity increases with an increase in Gc at the lower wall side. The variation of Nb on velocity distribution is shown in 3. It is noticed that velocity is not symmetric about the central line of the channel due to curvature.

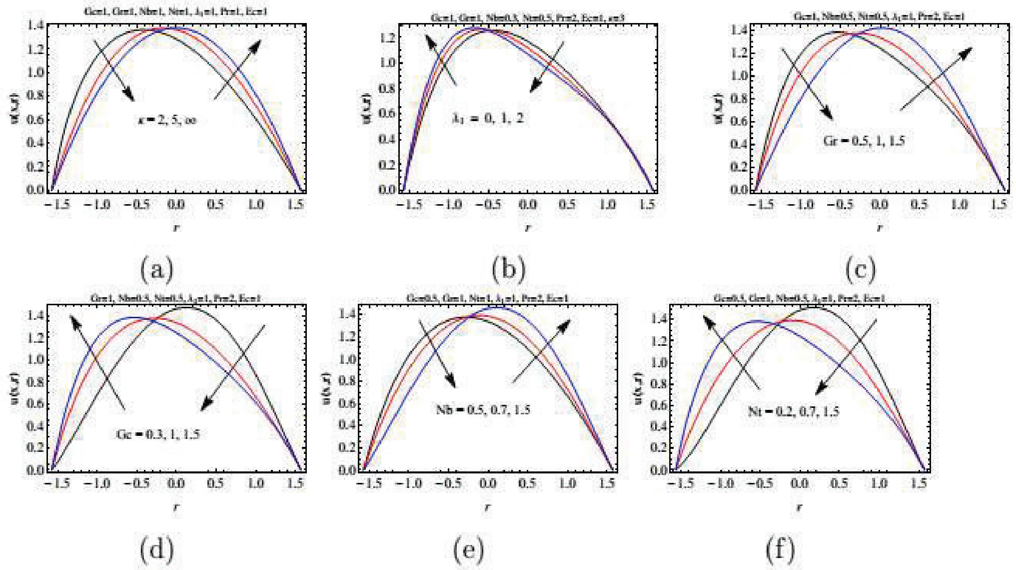

Figure 2: Variation of $u(x,r)$ with $x = 0.1, \phi = 0.6, Q_T = 1.75$ and $t = 0.05$.

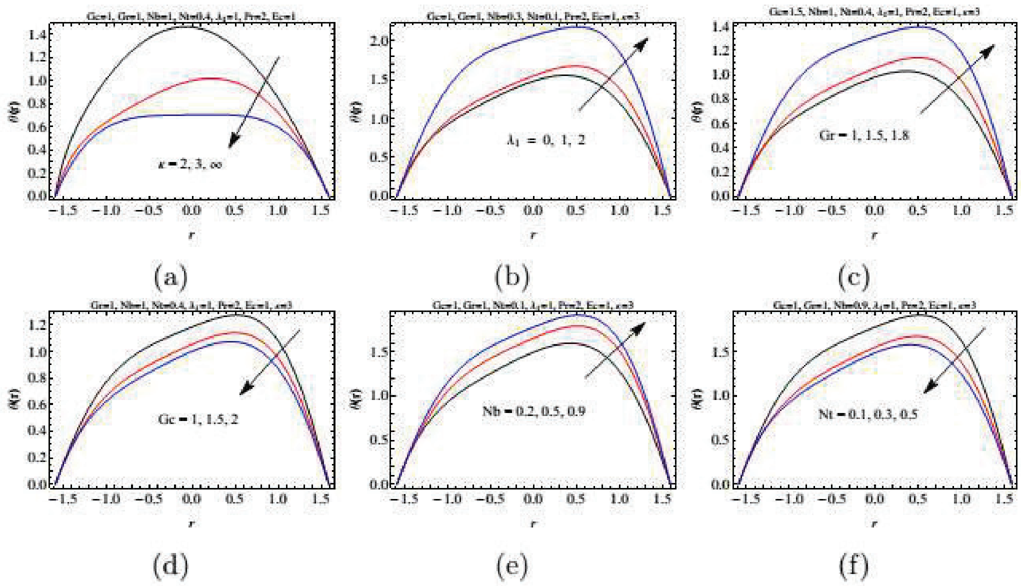

Figure 3: Variation of $\theta(r)$ with $x = 0.02, \phi = 0.6, Q_T = 1.5$ and $t = 0.05$.

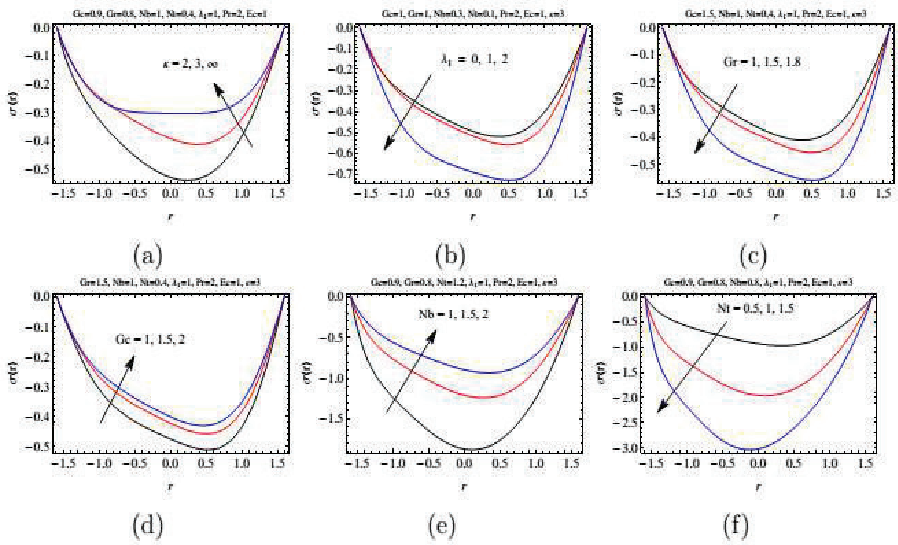

Figure 4: Variation of $\sigma(r)$ with $x = 0.02, \phi = 0.6, Q_T = 1$ and $t = 0.05$.

3.2 Temperature distribution

The variation of temperature distribution for different values of curvature parameter κ, Jeffrey fluid parameter λ_1, local temperature Grashof number Gr, local nanoparticle Grashof number Gc, Brownian motion parameter Nb, and thermophoresis parameter Nt are illustrated in figure 3.2. It is noticed that the pattern of the temperature profiles are parabolic and the fluid's temperature increases in the central line of the channel. This increase is due to the presence of viscous dissipation term, the viscosity of the fluid in the viscous fluid flow will get kinetic energy from the motion of the fluid and converted it into internal energy of the fluid that raises the fluid's temperature. This process is called viscous dissipation. Figure 3.1 discuss that the temperature profile is symmetric in the straight channel (i.e., for large curvature parameter κ), whereas the distributions are not symmetric in curved channel (i.e., for small curvature parameter κ). We also noticed that an increase in κ, decreases θ i.e., the curvature parameter highly affects the temperature distribution. Increase in Jeffrey fluid parameter enhances the temperature, see in figure 3.1. By increasing the λ_1 (ratio of relaxation time to retardation time) the relaxation time increases and the retardation time decreases that raises temperature. The effects of temperature Grashof number and nanoparticle Grashof number on the temperature are considered in figures 3.1 and 3.1. It is illustrated that the temperature increases with increase of Gr and decreases with Gc, i.e. the buoyancy forces due to temperature difference Gr and the buoyancy forces due to concentration difference Gc have opposite behaviors on the heat transfer distribution. From figures 3.1 and 3.1 we can see the behaviors of Nb and Nt. We understand that temperature increases with an increase in the Brownian motion parameter and decreases with the thermophoresis parameter. The enhancement of Brownian motion parameter leads to increase the kinetic energy of the nanoparticles and transforms it into internal energy that raises nanofluid's temperature. It is also observed that temperature distribution is not symmetric. this is due to the curvature effects in the curved channel (small curvature parameter κ).

3.3 Mass transfer distribution of nanoparticles

The concentration of nanoparticles for various parameters is examined through figures 3.2 to 3.2. we noticed a similar trend that the effect of a parameter on concentration of nanoparticles is relative to the effect of that parameter on temperature. Figure 3.2 shows that the concentration distribution increases with an increase in κ, i.e. the concentration distribution is low in curved channel and is high in straight channel. It is also observed that the distribution is not symmetric in curved channel, whereas for large value of κ (straight channel) the distribution is symmetric in the channel. Concentration of nanoparticles decreases with an increase in λ_1 (see figure 3.2). From figures 3.2 and 3.2, it can be illustrated that the concentration distribution decreases with an increase in Gr and increases with Gc. It is also noticed that the profiles are not symmetric. This is due to the curvature effects in the channel for small curvature parameter. Figure 3.2 depicts, significant increase in the concentration of nanoparticles when the value of Brownian motion parameter increases. The influence of thermophoresis parameter on concentration of nanoparticles is shown in figure 3.2. It is found that the effect of Nt is opposite to Nb. It is also found that the distribution profiles are not symmetric and the distribution attains maximum value at the walls of the channel.

4. Concluding Remarks

The peristaltic transport of Jeffrey nanofluid under the consideration of buoyancy and viscous dissipation effects in a curved channel is studied. Long wave length and low Reynolds number approximations are used and then the nonlinear coupled equations are solved using MATHEMATICA. The results for the case of Newtonian fluid in curved channel can be recovered by taking $\lambda_1 \to 0$. The present graphical results agree with the previous study of [10]. The results for the case of Newtonian fluid flow in a straight channel can be recovered by choosing $\lambda_1 \to 0$ and $\kappa \to 0$. The results are in good agreement with the previous studies.

References

[1] H. Sato, T. Kawai, T. Fujita, and M. Okabe. Two dimensional peristaltic flow in curved channels. Trans. Jpn. Soc. Mech. Eng., Ser. B 66 (2000) 679–685.

[2] N. Ali, M. Sajid, and T. Hayat. Long wave length flow analysis in a curved channel. Z. Naturforsch, 65a (2010a) 191–196.

[3] N. Ali, M. Sajid, T. Javed, and Z. Abbas. Heat transfer analysis of peristaltic flow in a curved channel. Int. J. Heat Mass Transfer, 53 (2010b) 3319–3325.

[4] T. Hayat, S. Noreen, and A. Alsaedi. Effect of an induced magnetic field on peristaltic flow of non-newtonian fluid in a curved channel. J. of Mechanics in Medicine and Biology, 12 (2012)1250058(1–26).

[5] N. Ali, M. Sajid, T. Javed, and Z. Abbas. An analysis of peristaltic flow of a micropolar fluid in a curved channel. Chin. Phys. Lett., 28 (2011) 014704(1–4).

[6] A. Kalantari, A. Riasi, and K. Sadeghy. Peristaltic flow of giesekus fluids through curved channels: an approximate solution. Nihon Reoroji Gakkaishi (Journal of the Society of Rheology, Japan), 42 (2014)9–17.

[7] J. V. Ramanamurthy, K. M. Prasad, and V. K. Narla. Unsteady peristaltic transport in curved channels. Phys. Fluids, 25 (2013) 091903(1–20).

[8] S. Hina, M. Mustafa, S. Abbasbandy, T. Hayat, and A. Alsaedi. Peristaltic motion of nanofluid in a curved channel. ASME Journal of Heat Transfer, 136 (2014) 052001(1–7).

[9] N. S. Akbar and S. Nadeem. Endoscopic effects on peristaltic flow of a nanofluid. Commun. Theor. Phys., 56(4) (2011) 761–768.

[10] N. S. Akbar, S. Nadeem, T. Hayat, and A. A. Hendi. Peristaltic flow of a nanofluid with slip effects. Meccanica, 47(5) (2012a) 1283–1294.

[11] N. S. Akbar, S. Nadeem, T. Hayat, and A. A. Hendi. Peristaltic flow of a nanofluid in a non-uniform tube. Heat Mass Transfer, 48 (2012b) 451–459.

[12] N. S. Akbar and S. Nadeem. Peristaltic flow of a phan-thien-tanner nanofluid in a diverging tube. Heat Transf Res, 41 (2012c) 10–22.

[13] S. Akram, S. Nadeem, A. Ghafoor, and C. Lee. Consequences of nanofluid on peristaltic flow in an asymmetric channel. Int J Basic Appl Sci IJBAS-IJENS, 12(5) (2012) 75–96.

[14] D. Tripathi and O. Anwar Beg. A study on peristaltic flow of nanofluids: Application in drug delivery systems. International Journal of Heat and Mass Transfer, 70 (2014) 61–70.

[15] M. Kothandapani and J. Prakash. Influence of heat source, thermal radiation and inclined magnetic fiels on peristaltic flow of a hyperbolic tangent nanofluid in a trapered asymmetric channel. IEEE Transactions on NanoBioscience, 99 (2014) 1–12.
[16] S. Nadeem, E. N. Maraj, and N. S. Akbar. Investigation of peristaltic flow of williamson nanofluid in a curved channel with compliant walls. Appl Nanosci., 4 (2014) 511–521.